

Corrosion Protection Study for Carbon Steel in Seawater by Coating with SiC and ZrO₂ Nanoparticles

Khulood Abid Saleh Al-Saadie¹, Haider A. Yousif Al-Mashhdani^{2,*}

¹University of Baghdad, College of Science, Department of Chemistry, Baghdad, Iraq

²Al-Rasheed University College, Department of Dentistry, Baghdad, Iraq

Abstract The corrosion protection by coating carbon steel (C.S) with SiC and ZrO₂ NPs was investigated in presence of different Polyacrylic acid (PAA) concentration. Electrophoretic deposition (EPD) method using was applied ethanol suspensions and polyacrylic acid (PAA) as stabilizing agent. The deposition of SiC and ZrO₂ NPs was occurred on the carbon steel (C.S) alloy as cathode. Coated C.S by NPs in presence of PAA revealed a good corrosion protection efficiency even at temperature ranged (298- 328)K in seawater (3.5% NaCl). Results show that using PAA in suspension coat increased PE% when compared with PE% in absence of PAA and gives resistance in above temperature range. Kinetic parameters (activation energy and pre-exponential factor) were calculated and discussed. Also, thermodynamic Values ΔG and ΔH were calculated and it shows that corrosion reaction was spontaneous and exothermic in nature. The surface morphology was examined by AFM techniques; the resulted AFM images were detect the morphology of surface and the particles size of coat layers which range from 60-103 nm.

Keywords Corrosion protection, Coating, SiC Nanoparticles, ZrO₂ NPs, PAA

1. Introduction

Corrosion is an electrochemical phenomenon and is accompanied by the flow of electrical current and its degradation of materials and structures is one of the important issues that lead to depreciation of investment goods. The damages by corrosion generate not only high costs for inspection, repairing and replacement, but in addition these constitute a public risk [1]. Seawater (3.5% NaCl) solutions are widely used in industry, which leads to corrosive attack. The corrosion protection by coats is one of the most common effective and economic methods to protect metals in acid media [2-8]. Nanomaterials are important due to their unique properties that may lead to new and exciting applications. Nanoparticle coatings possess good thermal and electrical properties and they are resistant to oxidation, corrosion, erosion and wear in high temperature environments [9]. These property is very important factor in the applications such as pipelines, castings and automotive industry.

Electrophoretic deposition (EPD) is a simple method for the formation of a coating nanomaterials on an electrode using a stable suspension in a direct current (DC) field [10, 11]. EPD technique was used to coat silicon carbide

(SiC) particles on metal surfaces. Both sparse SiC particles and dense particle coating layers were fabricated on metal surface. Detailed analysis shows that SiC particles are bonded and compacted well with the metal surface [12], also used Zirconium oxide (ZrO₂) [13] & alumina (Al₂O₃) [14] nanoparticles lead to similar layers.

However, in aqueous-based EPD suspensions, method presented several disadvantages, for example, corrosion of the electrodes and gas bubbles produced by electrolysis of water at the electrodes during the EPD, which would reduce the density of deposited layer [15-18]. To avoid the formation of gas bubbles, non-aqueous suspensions became a preferred choice. Among the non-aqueous media, ethanol was the common dispersing medium for EPD [19]. In this research, ethanol was used as a solvent for EPD because of its less toxicity, less harmfulness to the environment, and good volatility.

EPD modified by using polymer as charging and stabilizing agent, acted effectively as colloidal particles during EPD [20]. Electrophoretic deposition (EPD) with ethanol as suspension medium and poly(acrylic acid) (PAA) as polymeric charging agent give good protection. In addition, the suspension must possess a high stability, thus charged polymers and surfactants were added to the suspension [21-23]. These additives, which were adsorbed onto the surfaces of ceramic particles, could generate steric and electrostatic stabilization and prevent particles agglomeration [24].

* Corresponding author:

H_r200690@yahoo.com (Haider A. Yousif Al-Mashhdani)

Published online at <http://journal.sapub.org/chemistry>

Copyright © 2015 Scientific & Academic Publishing. All Rights Reserved

2. Materials and Methods

2.1. Materials

The steel used in this study is a carbon steel (C45) with a chemical composition (in wt%) of 0.42% C, 0.40 % Si, 0.50% Mn, 0.045% S, 0.40% Cr, 0.045% P, 0.40% Ni, 0.01% Mo and the remainder is iron (Fe). The carbon steel samples were pre-treated prior to the experiments by grinding with emery paper SiC (120, 600 and 1200); rinse with distilled water, degreased in acetone, washed again with distilled water and then dried at room temperature before used synthesized seawater. The seawater solution was prepared by dissolved 35 g NaCl in 1L distilled water. SiC Nanoparticles were used in size range (20-30nm, Hongwu nanometer, purity 99.9%), ZrO₂ (40-50nm, Hongwu nanometer, purity 99.9%) and iodine was used in 99.8% purity (Aldrich).

2.2. Preparation of Emulsion Solution

Emulsion solution was prepared by adding 1% nanoparticles (NPs) (ZrO₂ or SiC) powder to ethanol as solvent [25] (adding 1.5 g NPs to 150 ml ethanol). To study the effect of adding different PAA% (0.1, 0.25, 0.5 & 1%) in emulsion solution (0.1, 0.25, 0.5, 1)g of PAA was added to in 100 ml ethanol respectively.

To homogenize the solution, an ultrasonic (50W) stirrer was used to mixed the solution for 30 min. The solutions were applied for coating carbon steel (C45) pieces by using EPD technique method. Sometime few I₂ were added to increase conductivity [26].

2.3. Electrophoresis Deposition of Emulsion Solution (Coating Samples)

To deposit emulsion solution on a piece of carbon steel surfaces, deposition cell device was used. The electrodes were connected to a D.C power supply; it can be used in anodic or cathodic deposition by reversing electrodes of the power supply [27]. The deposition cell device composed of the following components:

1. Beaker 250 ml capacity and cover contain two slit with distance between then equal to 1cm.
2. Power supply used to supply constant direct current D.C voltage (0 – 20) V.
3. An electrical circuit was connected by ammeter, respectively, to measure the current generated between the poles.
4. Stainless steel rode used as inert electrode in deposition process cell [28].
5. A piece of carbon steel catch by tong made of stainless steel fixed with 1cm distance between it and inert electrode.

The deposition on C.S specimens were carried for (3,4,5 and 6) minutes, then all specimens thermally dried at 150°C for 2 min.

2.4. Electrochemical Measurements

The electrochemical measurements were carried out using Mlab (Germany, 2000) potentiostat and controlled by computer and MLabSci software which were used for data acquisition and analysis under static condition. The corrosion cell used had three electrodes, the reference electrode was a silver-silver chloride, platinum electrode was used as auxiliary electrode with 1 cm² surface area of and the working electrode was carbon steel. All potentials given in this study were referred to this reference electrode. The working electrode was immersed in test solution for 15 minutes to a establish steady state open circuit potential (E_{ocp}), then electrochemical measurements were performed in potential range (± 200) mV. All electrochemical tests have been performed in aerated solutions at (208-328) K.

3. Result and Discussion

3.1. Polarization Curve

Figure (1) shows the polarization curves of carbon steel coated with SiC and ZrO₂ NPs in presence of various PAA%. It could be observed that both the cathodic and anodic reactions were suppressed with the addition of different PAA%, which suggests that coated by SiC and ZrO₂ in presence of different PAA% reduced anodic dissolution and also retarded the oxygen reduction reaction effectively. Protection efficiencies (PE%) of all types of coating estimated by comparison with the measurements of the uncoated surface of carbon steel alloy using equations (1):

$$PE\% = \frac{(i_{corr})_{uncoated} - (i_{corr})_{coated}}{(i_{corr})_{uncoated}} \times 100 \quad (1)$$

Where PE%; protection efficiency percentage, i_{corr} (uncoated) and i_{corr} (coated); are corrosion current densities for uncoated and coated specimen respectively.

To measure the thickness of coat layer on C.S surface, the basic following equation can be used:

$$\rho = \frac{wt}{V} \quad (2)$$

Where: ρ = density of NPs, Wt.= weight of coated and V= volume of coated.

$$V = r^2 * 3.14 * d \quad (3)$$

Where: r = radius of C.S piece and d = thickness of coated.

3.2. Effect of PAA %

Effect of different PAA concentration in the SiC NPs suspension solution, were investigated, PAA lead to increase the stability of suspension solution and increase the thickness of SiC NPs coat, with increase concentration of PAA in suspension. Adding 0.25% of PAA for the suspension of SiC coating lead to the lowest i_{corr} value in temperature range (298- 328)K, as shown in figure (2-a).

The corrosion potential (E_{corr}) is shifted to the highest

noble potential (positive direction) when C.S coated by SiC NPs with (0.25%) PAA. The protection efficiency for C.S specimens coated by SiC NPs in presence of different PAA% in seawater at different temperatures (298, 308, 318, 328)K were investigated, and the best PE% was obtained in

presence of (0.25%) PAA at 298K. So (0.25%) PAA was perfect concentration added to suspension solution of coating which give PE% range between (99.65 – 96.7%) at temperatures range 298- 328 K, as shown in fig.2.

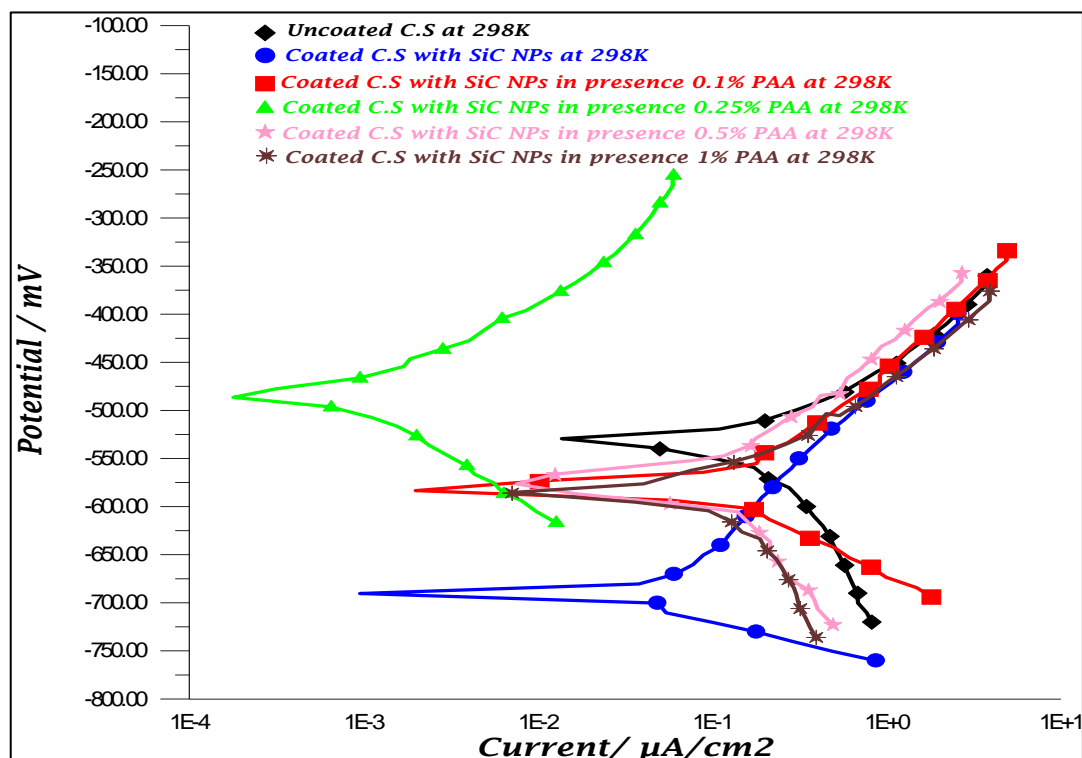


Figure 1a. Polarization curves for C.S in 3.5% NaCl for uncoated and coated C.S with SiC NPs in absence and percent of different PAA%

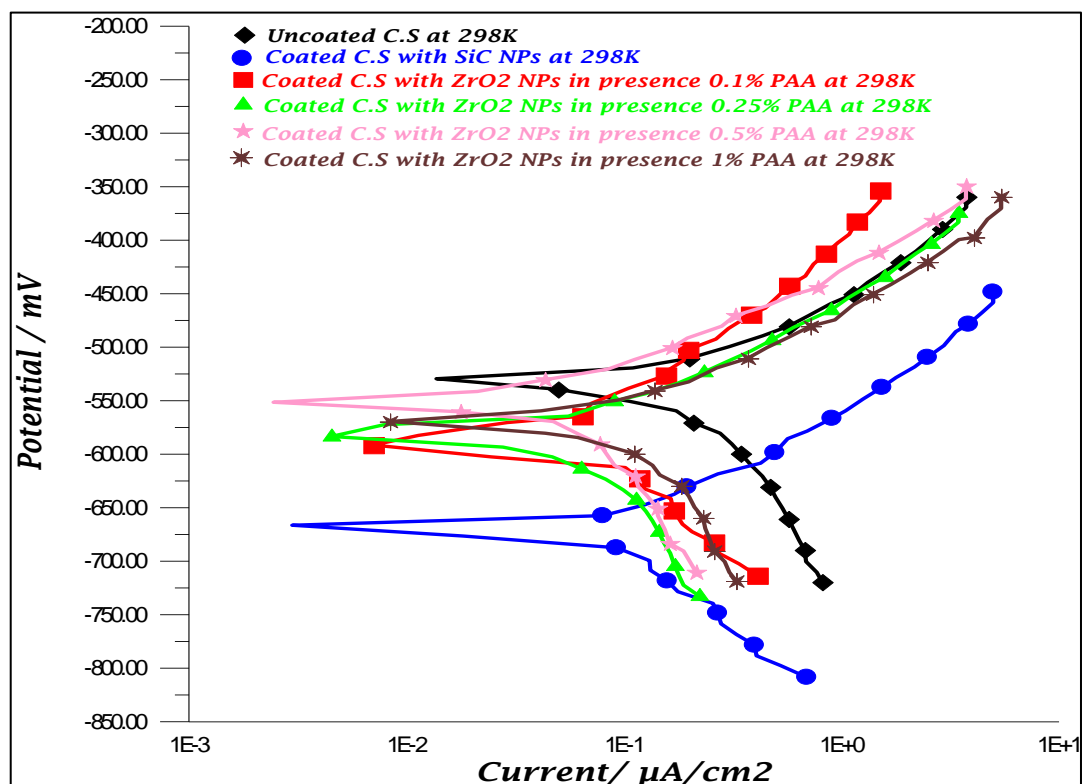


Figure 1b. Polarization curves for C.S in 3.5% NaCl for uncoated and coated C.S with ZrO₂ NPs in absence and percent of different PAA%

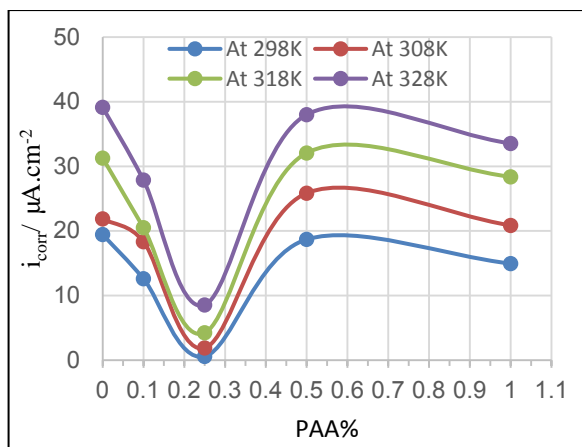


Figure 2a. Effect of adding different PAA% to SiC NPs coating suspension on i_{corr}

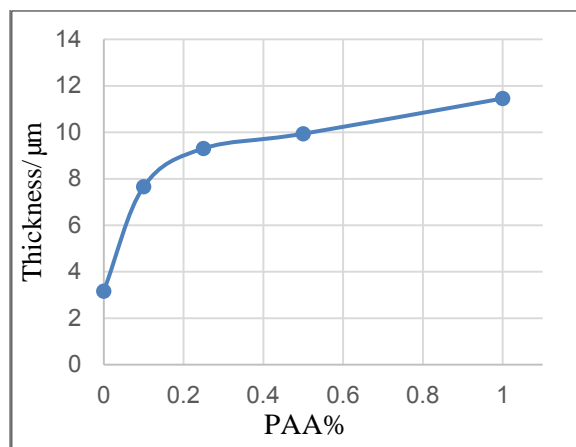


Figure 2d. Effect of adding different PAA% to SiC NPs coating suspension on thickness of coat

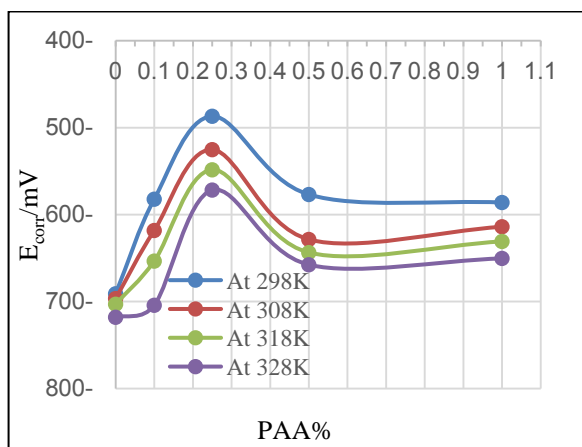


Figure 2b. Effect of adding different PAA% to SiC NPs coating suspension on E_{corr}

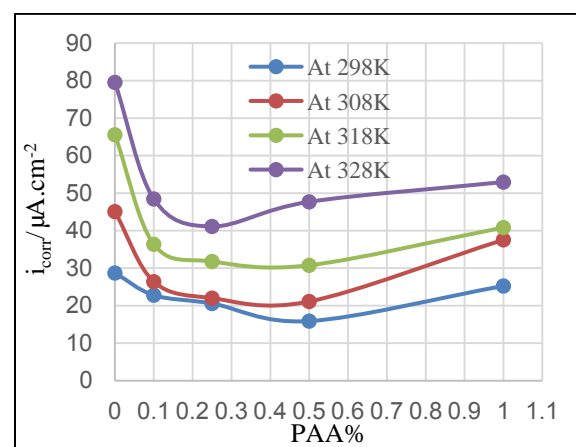


Figure 3a. Effect of adding different PAA% to ZrO_2 NPs coating suspension on i_{corr}

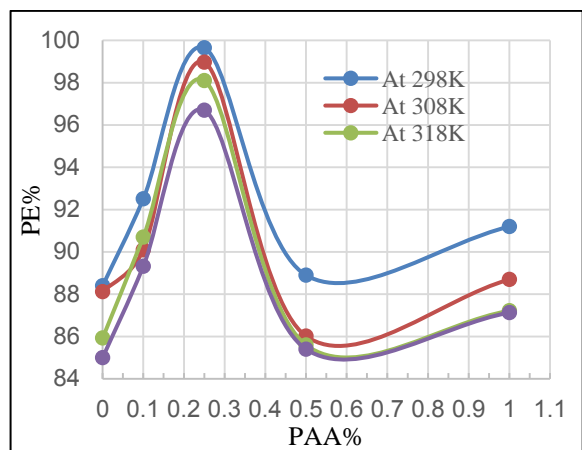


Figure 2c. Effect of adding different PAA% to SiC NPs coating suspension on PE%

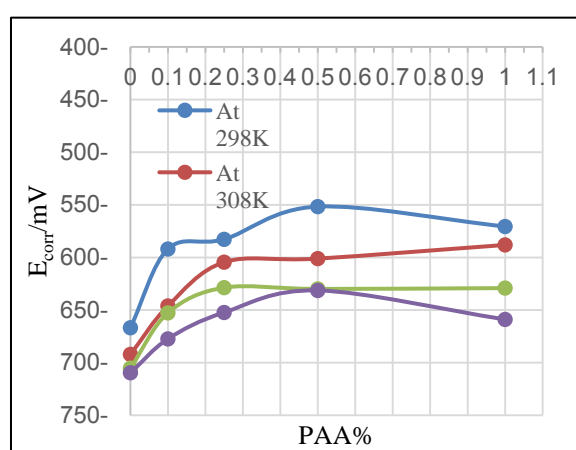


Figure 3b. Effect of adding different PAA% to ZrO_2 NPs coating suspension on E_{corr}

Adding different PAA% in suspension of ZrO_2 give different thickness coated, and (0.5%) PAA give the highest thickness (12.6 μm). Different PAA% lead to thickness ranged between (5.3- 12.6 μm), as shown in figure (3-d).

I_{corr} value were reduced after coated with ZrO_2 NPs in presence of PAA, and the lowest value was obtained with (0.5%) PAA at 298K as shown in figure (3-a), while values of E_{corr} for C.S coated by ZrO_2 NPs in absence and presence

of different PAA% were shifted to more negative potentials with increasing temperature, as shown in figure (3-b). The protection efficiency (PE%) slightly decreased, when temperatures increased, the best (PE%) obtained at 298K with (0.5%) PAA which was (91.2%), while at other PAA% and temperatures the (PE%) ranged between (79-89)%. This could be explained that the PAA increasing the coated efficiency by ZrO₂ on C.S.

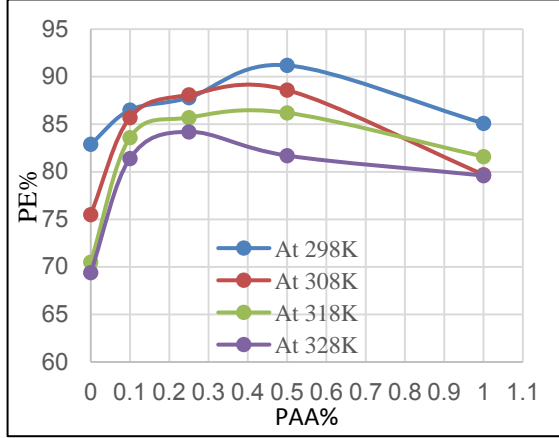


Figure 3c. Effect of adding different PAA% to ZrO₂ NPs coating suspension on PE%

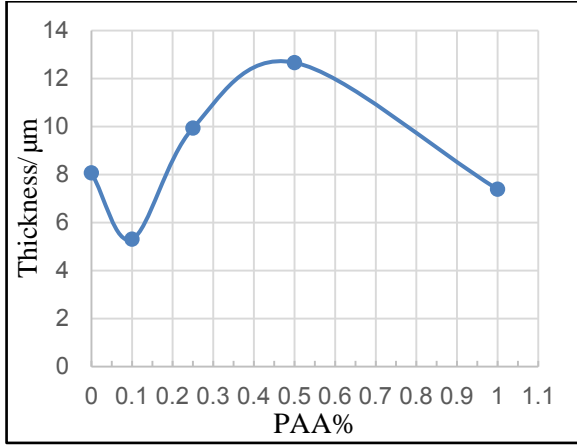


Figure 3d. Effect of adding different PAA% to ZrO₂ NPs coating suspension on thickness of coat

The corrosion of all Coated suspension by SiC NPs in absence and presence of variation PAA% were have little dependence on temperatures except coated by SiC without PAA havn't dependence on temperature, while coated by ZrO₂ NPs in absence and presence different PAA% were have more dependence on temperature, only ZrO₂ without PAA and ZrO₂ with (1%) PAA coated were dependent on temperature, as shown in figure (4-b).

3.3. Surface Porosity

Surface porosity percentage fraction was estimated by potentiostatic polarization. In this case, the porosity percentage (*P*%) can be calculated using the following equation:

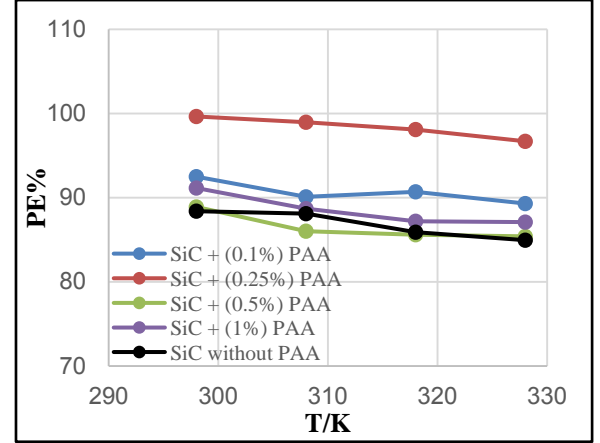


Figure 4a. Effect of temperature on PE% of C.S coated by SiC NPs in absence and presence different PAA%

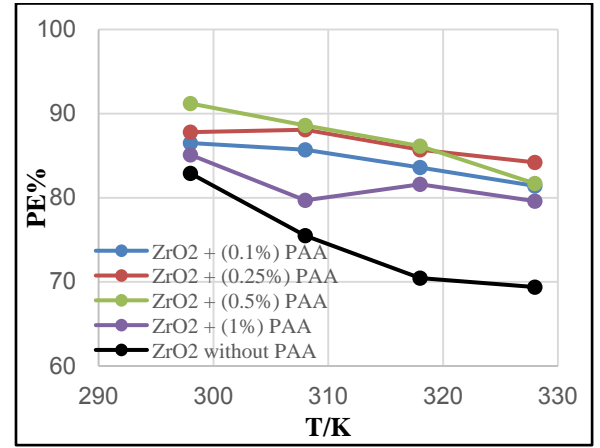


Figure 4. Effect of temperature on PE% of C.S coated by a) SiC NPs and b) ZrO₂ in absence and presence different PAA%

$$P\% = \frac{R_{p,uncoated}}{R_{p,coated}} 10^{-\left(\frac{\Delta E_{corr}}{\beta_a}\right)} \times 100 \quad (4)$$

where $R_{p,uncoated}$ and $R_{p,coated}$ are the polarization resistances of the uncoated C.S and the coating C.S by NPs, respectively, ΔE_{corr} is the corrosion potential difference between them, and β_a is the anodic Tafel coefficient of the uncoated C.S.

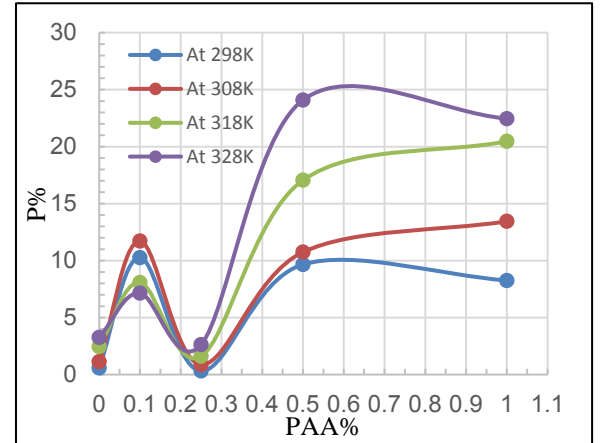


Figure 5a. Variation of porosity percentage *P*% with PAA% at different temperatures for C.S coated by SiC NPs in absence and presence of different PAA%

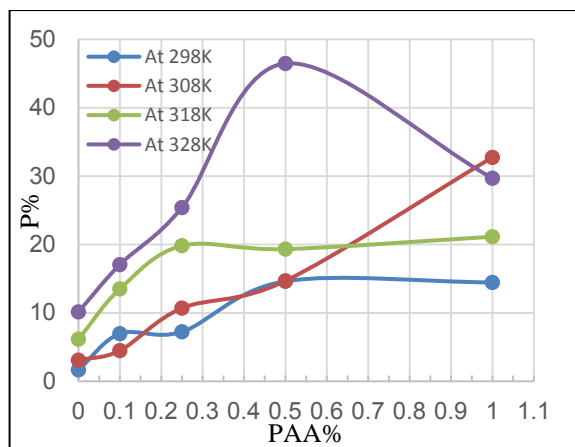


Figure 5b. Variation of porosity percentage P% with PAA% at different temperatures for C.S coated by ZrO₂NPs in absence and presence of different PAA%

In generally adding PAA increase surface porosity percentage (P%) for coated C.S by SiC NPs except at 0.25% PAA were P% decrease, 0.5% PAA lead to higher P% which reach to 24.09% at 328K. Adding different PAA% increase the surface porosity percentage of coated C.S by ZrO₂. The P% values for C.S coated by ZrO₂ in the presence of various PAA% give higher P% values as comparison with P% values in absence of PAA, as shown in figure (5).

3.4. The Kinetic Studies

The effect of temperature on the rate of C.S corrosion has been studied over the temperature range (293-308)K. Figure (6) shows $\log i_{\text{corr}}$ plotted against the reciprocal of the absolute temperature ($1/T$) for the corrosion of coated and uncoated C.S alloy and with adding different PAA%.

The relation was almost linear dependence between the corrosion rate ($\log i_{\text{corr}}$) and $1/T$ which can be expressed as: [29]

$$\log i_{\text{corr}} = \log A - E_a / 2.303 RT \quad (5)$$

Where R is the gas constant ($R \approx 8.314 \text{ J K}^{-1} \text{ mol}^{-1}$)

This relation is similar to the well-known Arrhenius equation with

$$r = A \exp(-E_a/RT) \quad (6)$$

E_a represents the activation energy of the corrosion and A is the pre-exponential factor in the rate equation. Values of E_a and A are then derived from the slope and the intercept of the $\log i_{\text{corr}}$ versus $1/T$ plot respectively as shown in figure (6). Table (1) presents E_a and the pre-exponential factor (A) values for the C.S alloy.

Adding 0.25% of PAA for SiC NPs suspension lead to increase E_a from 20.104 $\text{kJ} \cdot \text{mol}^{-1}$ to 71.936 $\text{kJ} \cdot \text{mol}^{-1}$ which mean that 0.25% PAA lead to decreased the corrosion rate more than other PAA%, where E_a values range (19.105 – 22.270) $\text{kJ} \cdot \text{mol}^{-1}$. The value of A remain generally the same in absence and presence of PAA.

The activation energy E_a increases in presence of 0.5% PAA and reach to (29.758) $\text{kJ} \cdot \text{mol}^{-1}$ and the lowest E_a value are with 1% PAA (18.802) $\text{kJ} \cdot \text{mol}^{-1}$, which is lower than E_a for the corrosion of C.S coated by ZrO₂ without presence of

PAA (28.491) $\text{kJ} \cdot \text{mol}^{-1}$.

Table 1. Kinetic parameter for C.S coated with SiC and ZrO₂ in absence and presence of different PAA% in 3.5% NaCl

| | Conc. | $E_a/\text{kJ} \cdot \text{mol}^{-1}$ | $A/\text{Molecules} \cdot \text{cm}^{-2} \cdot \text{s}^{-1}$ |
|----------------------------|-------------|---------------------------------------|---|
| | Uncoated | 12.330 | $1.32 \cdot 10^{28}$ |
| Coated by SiC | Without PAA | 20.105 | $3.271 \cdot 10^{28}$ |
| | (0.1%) PAA | 20.277 | $2.807 \cdot 10^{28}$ |
| | (0.25%) PAA | 71.936 | $2.807 \cdot 10^{28}$ |
| | (0.5%) PAA | 19.105 | $2.593 \cdot 10^{28}$ |
| | (1%) PAA | 22.270 | $7.385 \cdot 10^{28}$ |
| Coated by ZrO ₂ | Without PAA | 28.491 | $1.492 \cdot 10^{30}$ |
| | (0.1%) PAA | 20.899 | $5.99 \cdot 10^{28}$ |
| | (0.25%) PAA | 19.756 | $3.33 \cdot 10^{28}$ |
| | (0.5%) PAA | 29.758 | $1.49 \cdot 10^{30}$ |
| | (1%) PAA | 18.802 | $3.15 \cdot 10^{28}$ |

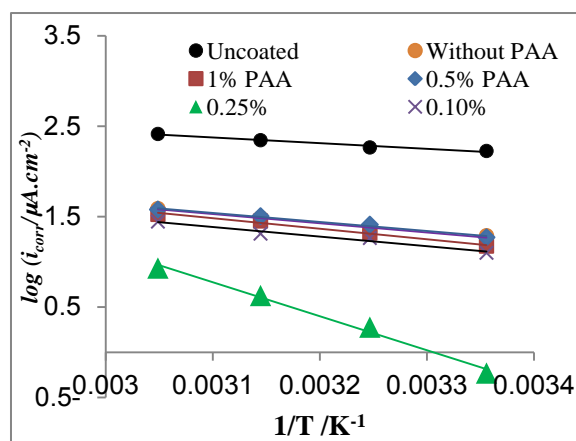


Figure 6a. $\log i_{\text{corr}}$ Vs $1/T$ for coated C.S with SiCNPs in absence and presence of different PAA% in 3.5% NaCl

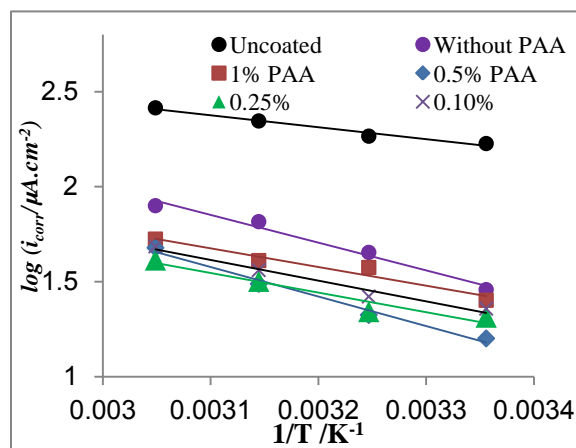


Figure 6b. $\log i_{\text{corr}}$ Vs $1/T$ for coated C.S with ZrO₂NPs in absence and presence of different PAA% in 3.5% NaCl

3.5. The Thermodynamic Studies

The change in Gibbs free energy (ΔG) for the corrosion of C.S alloy specimens at a given temperature may be estimated from the following equation:

$$\Delta G = -nFE_{\text{corr}} \quad (7)$$

Where n (which is considered equal to 2) is the number of electrons involved in the anodic process, from the values of ΔG at four different temperatures in the range 298-328 K, the change in the entropy (ΔS) of corrosion process could be derived using the well-known thermodynamic relation:

$$\Delta G = \Delta H - T\Delta S \quad (8)$$

Table (2) give the average values of the thermodynamic quantities ΔG , ΔS and ΔH for the corrosion of uncoated C.S and coated by SiC and ZrO₂ NPs in absence and presence of different PAA%.

Table 2. Thermodynamic parameter for coated C.S with SiC and ZrO₂ in absence and presence of different PAA% in 3.5% NaCl

| | Conc. | $-\Delta G_{\text{avg}}/\text{kJ.mol}^{-1}$ | $-\Delta H_{\text{avg}}/\text{kJ.mol}^{-1}$ | $-\Delta S/\text{J.K}^{-1}.\text{mol}^{-1}$ |
|----------------------------|-------------|---|---|---|
| Coated by SiC | Uncoated | 110.86 | 304.55 | 618.6 |
| | Without PAA | 135.51 | 188.34 | 168.8 |
| | (0.1%) PAA | 123.42 | 365.78 | 774.3 |
| | (0.25%) PAA | 102.87 | 270.47 | 536.3 |
| | (0.5%) PAA | 120.94 | 276.50 | 497.0 |
| | (1%) PAA | 119.71 | 246.44 | 404.9 |
| Coated by ZrO ₂ | Without PAA | 133.83 | 257.07 | 390.8 |
| | (0.1%) PAA | 123.92 | 282.67 | 507.2 |
| | (0.25%) PAA | 119.10 | 259.66 | 449.1 |
| | (0.5%) PAA | 116.48 | 278.30 | 517.0 |
| | (1%) PAA | 118.05 | 302.85 | 590.4 |

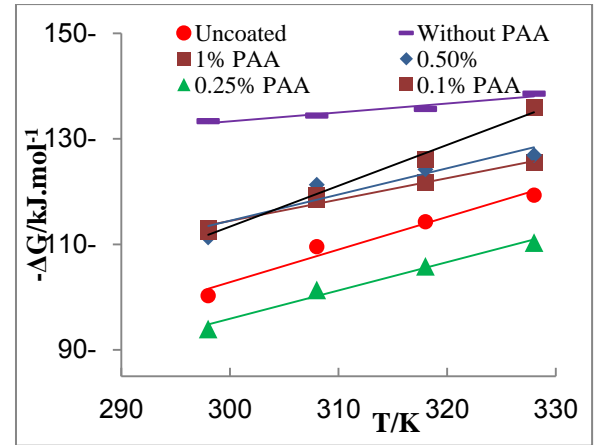


Figure 7a. Plot of $-\Delta G$ Vs T for coated C.S with SiCNPs in absence and presence of different PAA% in 3.5% NaCl

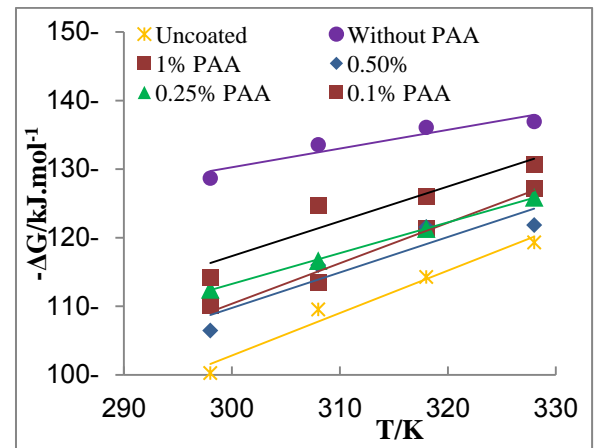


Figure 7b. Plot of $-\Delta G$ Vs T for coated C.S with ZrO₂NPs in absence and presence of different PAA% in 3.5% NaCl

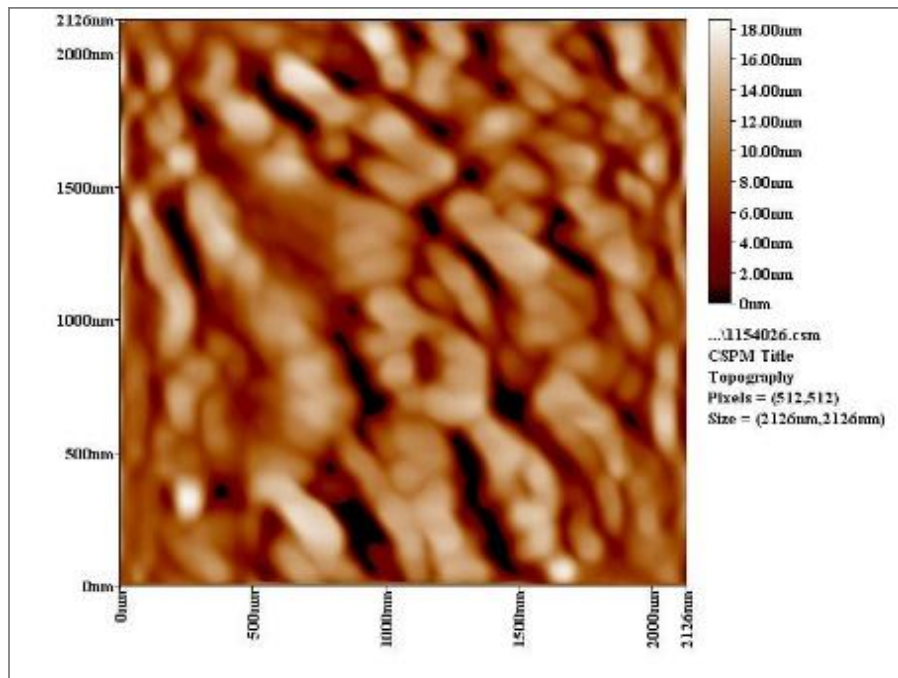


Figure 8a. AFM section line image of SiC without PAA

The results of table (2) express the thermodynamic feasibility of the corrosion reactions all of C.S. Values of ΔG was negative refer to the spontaneous corrosion reaction is spontaneous reaction. Values of ΔG for the corrosion of the C.S coated by SiC NPs in absence and presence of different PAA% increased after coated except coating in presence of (0.25%) PAA, while coated by ZrO_2 NPs lead to increased ΔG values in absence and presence of different PAA%, and the observed ΔG values decreased with PAA% increase.

The negative values of ΔH for corrosion processes in absence and presence of PAA reveal the exothermic nature of the carbon steel dissolution process.

Values of ΔS in presence of PAA are generally higher than for case without adding PAA, and there values increased generally with PAA increase.

3.6. The Surface Morphology

The results of the Surface Morphology Analysis by AFM for coated by SiC, are shown in figure (8). The average roughness of layer SiC NPs without PAA was calculated as 60 nm, which nearly three times greater than the stating particles (20nm), but layers SiC NPs in presence 0.25% PAA only, show a degree of agglomeration of the nanoparticles due to adhesiveness of SiC NPs with PAA and the produced layer are higher density greater adhesive with larger particles. The particle size distribution is tabulated in figure (8b and 8d), it showed that the average particles size around 95.26 nm.

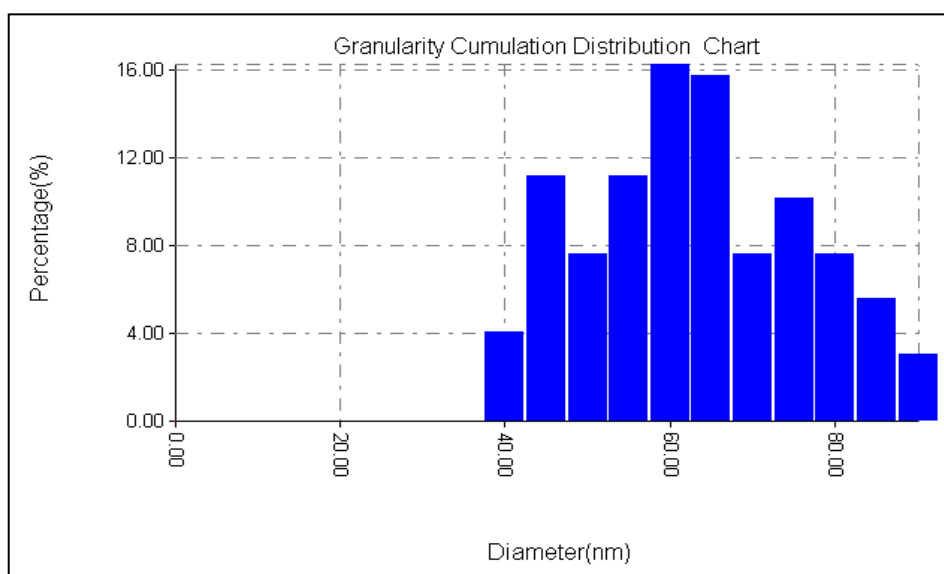


Figure 8b. Particle size distribution of SiC without PAA

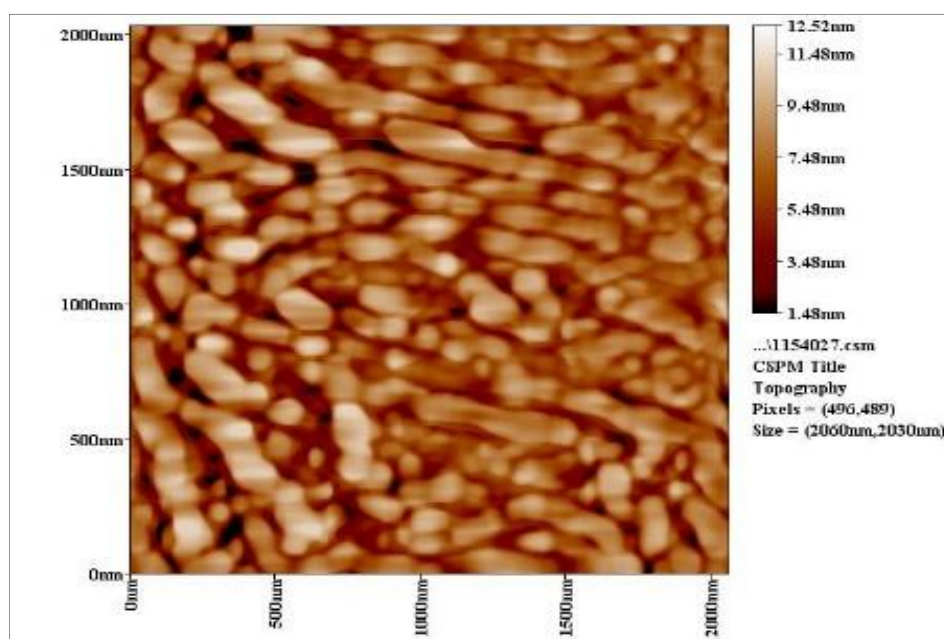


Figure 8c. AFM section line image of SiC with PAA

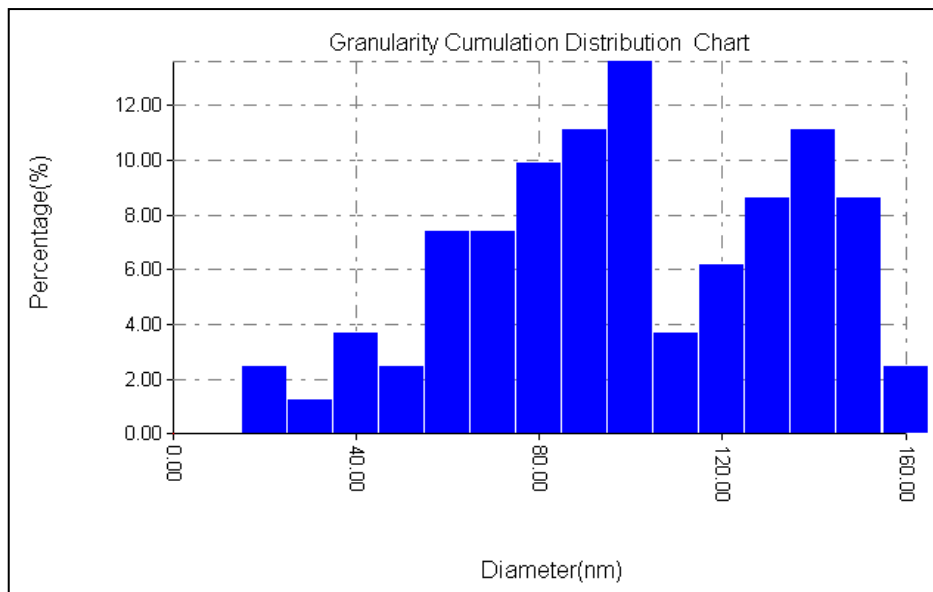


Figure 8d. Particle size distribution of SiC with PAA

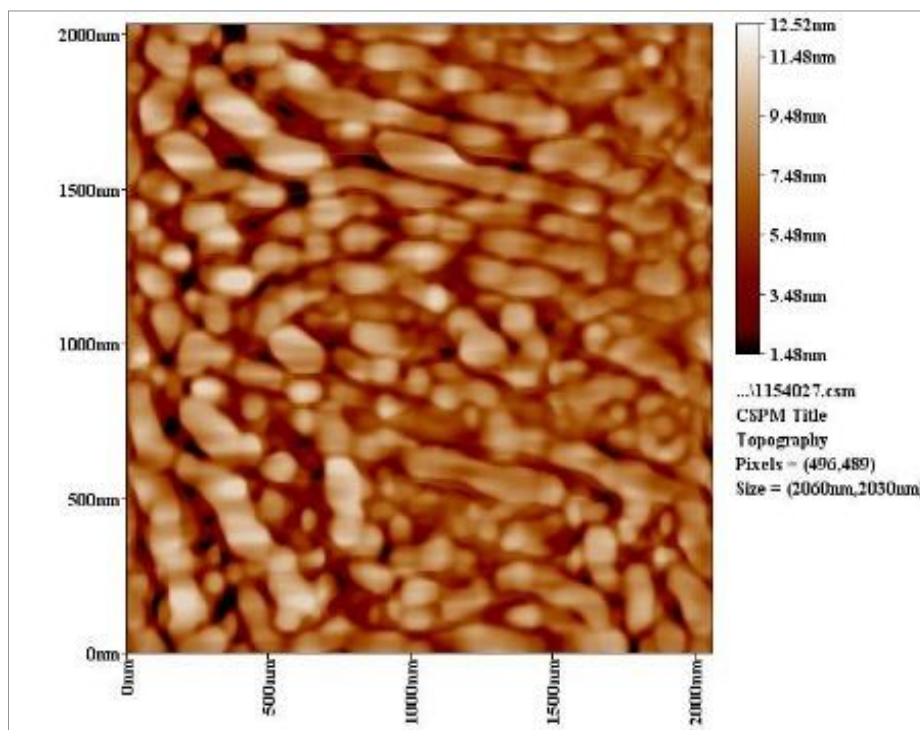


Figure 9a. AFM section line image of ZrO₂ without PAA

The AFM images for coated C.S by ZrO₂ in absence and presence PAA are shown in figure (9). Coated layers of ZrO₂ without PAA, this type seem to be smooth surfaces with grains greater than to the starting nano powder (40-50nm) after coat increase to the average particles size around (61 nm), figures (9a and 9b).

C.S Specimens coated with ZrO₂ with 0.5% PAA subjected to AFM analysis, figure (9c), revealed formation of large ZrO₂ particles with sizes exceeded 103nm.

4. Conclusions

1. The Electrophoretic Deposition (EPD) technique was successfully applied to coat C.S by SiC & ZrO₂ nanoparticles.
2. The protection efficiency of coated C.S by SiC NPs unaffected by temperatures but the protection efficiency for coated C.S by ZrO₂ NPs affected with temperatures.

3. Added PAA in the suspension solution act as stabilizing agent and create NPs coated more smooth and resist to heat.
4. The rate of corrosion increased with increasing temperatures ranged from 298 to 328 K.
5. After coated by NPs, Two important trends are evident. Firstly, the corrosion potential shifted toward more active value in coated carbon steel with NPs , Secondly, the corrosion current densities were significant reduced with coated by the two NPs.
6. The protected by coated with SiC NPs without PAA was more resistant to corrosion comparison with the protected by coated with ZrO_2 NPs.
7. PAA increased the protection when added in suspension solution of coated. And adding (0.25%) PAA in suspension solution of SiC NPs lead to highest protection efficiency.

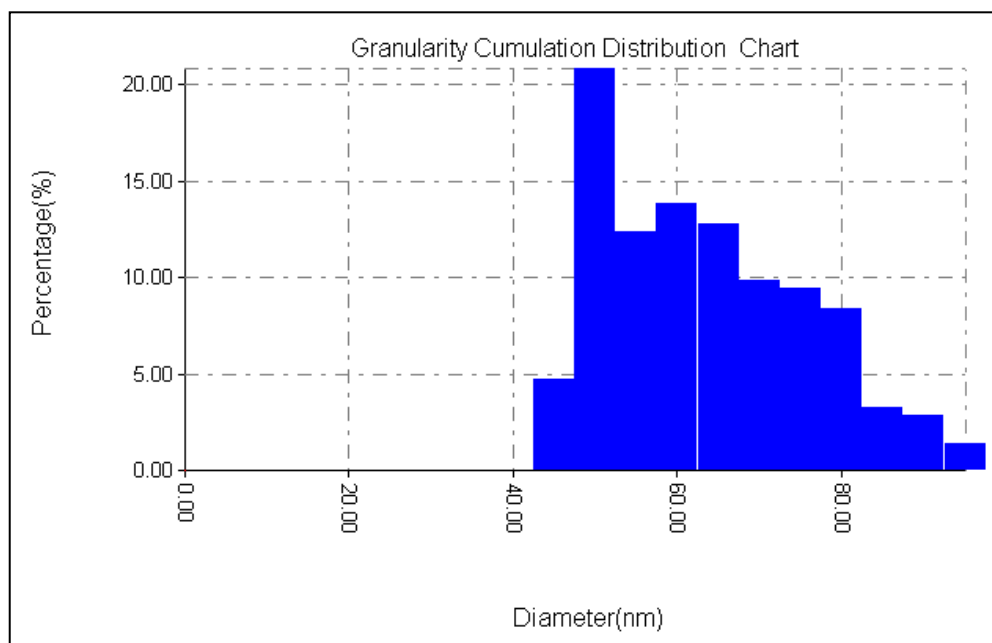


Figure 9b. Particle size distribution of ZrO_2 without PAA

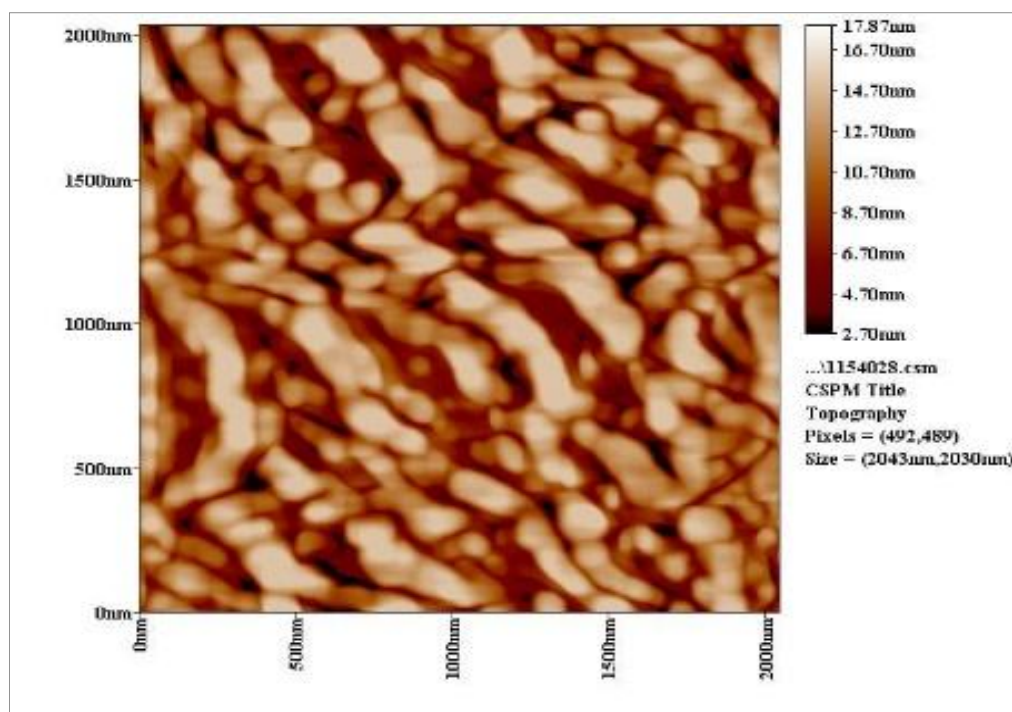


Figure 9c. AFM section line image of ZrO_2 with PAA

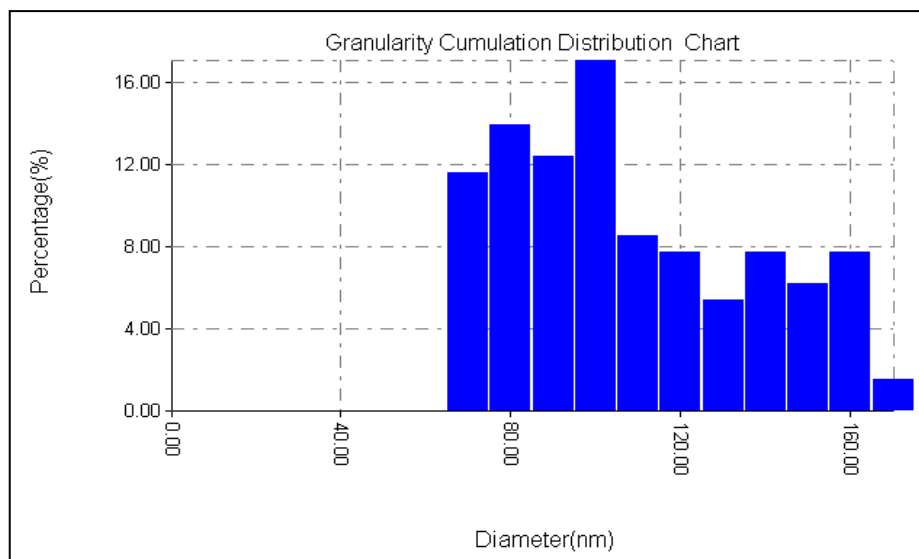


Figure 9d. Particle size distribution of ZrO₂ with PAA

8. The surface porosity percentage P%, generally increase with temperature increase, and adding different PAA% increase the P% because P% depended on R_p and E_{corr} .
9. The activation energy of C.S alloys corrosion increase after coated.
10. The corrosion reaction was spontaneous reaction (values of ΔG was negative) with exothermic reaction (values of ΔH was negative).
11. The AFM images detection The Particles size increase after coated by different NPs in all cases.

REFERENCES

- [1] Zheludkevich, M.; Shchukin, D.; Yasakau, K.; Mhwald, H; and Ferreira, M. G., 2007, Anticorrosion Coatings with Self-Healing Effect Based on Nanocontainers Impregnated with Corrosion Inhibitor, *Chem. Mater.* 19, 402-411.
- [2] Askari, E.; Mehrali, M.; Metselaar, I.H.S.C.; Kadri, N.A.; Rahman, Md. M., 2012, Fabrication and mechanical properties of Al₂O₃/SiC/ZrO₂ functionally graded material by electrophoretic deposition, *Journal Of The Mechanical Behavior Of Biomedical Materials*, 2, 144-150.
- [3] Yoshio, S. and Tetsuo, U., 2010, Forming and Microstructure Control of Ceramics by Electrophoretic Deposition (EPD), *KONA Powder and Particle Journal*, 28, 74-90.
- [4] Rasha, A.; Abdulkareem, M.; and Ahlam, M., 2014, corrosion protection studies of carbon steel and 316 stainless steel alloys coated by Nanoparticles, *Journal Baghdad for Science*, 11(1), 116-122.
- [5] Kretz, F.; Gaćsi, Z.; Kovaćs, J. and Pieczonka, T., 2004, The electroless deposition of Nickel on SiC particles for aluminum matrix composites, *Surface and Coatings Technology*, 180-181, 575-579.
- [6] Ferrari, B.; Sanchez-Herencia, A. and Moreno, R., 1998, aqueous electrophoretic deposition of Al₂O₃, ZrO₂ layered ceramics, *Materials Letters*, 35, 370-374.
- [7] Mišković-Stanković, V., 2012, Electrophoretic Deposition of Alumina And Boehmite Coatings On Metal Surfaces, *Macedonian Journal of Chemistry and Chemical Engineering*, 31(2), 183-193.
- [8] Dorian, A.; Marco, M.; Cristina L. and Charles, C., 2012, The effects of carboxylic acids on the aqueous dispersion and electrophoretic deposition of ZrO₂, *Journal of the European Ceramic Society*, 32(1), 235-244.
- [9] Saji, V. S. and Joice T., 2007, Nanomaterials for corrosion control, *current science*, 92(1), 51-55.
- [10] S. Mohammed Hassoni. M.Sc. Thesis, *University of technology* (Baghdad, Iraq, 2006).
- [11] Tang F., Uchikoshi T., Suzuki T., and Sakka Y., 2004, "Alignment of TiO₂ Particles by Electrophoretic Deposition in a High Magnetic Field", *Materials Research Bulletin*, 39(14-15), 2147-2154.
- [12] Zhao, B.; Wang, Y.; Liu, C.; Zhang, L.; Liu, X. and Zhang, Y., 2012, Ultrasonic nanowelding of SiC microparticles on Al surface, *Applied Surface Science*, 258(15), 5786- 5789.
- [13] Dorian A., Marco M., Cristina L. and Charles C. , 2012, The Effects of Carboxylic Acids on the Aqueous Dispersion and Electrophoretic Deposition of ZrO₂, *Journal of the European Ceramic Society*, 32(1), 235-244.
- [14] Askari E., Mehrali M., Metselaar I., Kadri N. and Rahman M., 2012, Fabrication and mechanical properties of Al₂O₃/SiC/ZrO₂ functionally graded material by electrophoretic deposition, *Journal of the Mechanical Behavior of Biomedical Materials*, 2, 144-150.
- [15] Moritz, T.; Eiselt, W. and Moritz, K., 2006, Electrophoretic deposition applied to ceramic dental crowns and bridges, *Journal of Materials Science*, 41, 8123-8129.
- [16] Christian O. and Rolf C., 2006, Preparation of zirconia dental crowns via electrophoretic deposition, *Journal of Materials Science*, 41, 8130-8137.

- [17] Maca, K., Hadraba, H. and Cihlar, J., 2004, Electrophoretic Deposition of Alumina and Zirconia: II. Two-Component Systems, *Ceramics International*, 30(6), 853-863.
- [18] Anne, G.; Vanmeensel, K.; Neirinck, B.; Vanderbiest, O. and Vleugels J., 2006, Ketone-amine based suspensions for electrophoretic deposition of Al_2O_3 and ZrO_2 , *Journal of the European Ceramic Society*, 26, 3531–3537.
- [19] Meng, S., Xiaojian, M., Jian, Z. and Shiwei, W., 2009, Electrophoretic shaping of sub-micron alumina in ethanol, *Ceramics International*, 35(5), 1855–1861.
- [20] Kok-Tee, L. and Sorrell, C., 2011, Electrophoretic Mobilities of Dissolved Polyelectrolyte Charging Agent and Suspended Noncolloidal Titanium during Electrophoretic Deposition, *Materials Science and Engineering: B*, 176 (5), 369-381.
- [21] Besra, L. and Liu, M., 2007, A Review on Fundamentals and Applications of Electrophoretic Deposition, *Progress in Materials Science*, 52, 1–61.
- [22] Riccardis, D.; Carbone, D. and Rizzo, A., 2007, A novel method for preparing and characterizing alcoholic EPD suspensions, *Journal of Colloid and Interface Science*, 307, 109–115.
- [23] Novak, S. and Konig K., 2009, Fabrication of alumina parts by electrophoretic deposition from ethanol and aqueous suspensions, *Ceramics International*, 35, 2823–2829.
- [24] Chun-mei, Y., Xian-chun, C., Xiaoming, L., Zhong-bing, H., Ya-dong, Y. and Guang-fu Y., 2011, Electrophoretic deposition of $\text{Al}_2\text{O}_3/\text{ZrO}_2$ layer with controllable thickness in ethanol medium, *Frontiers of Chemistry in China*, 6(2), 76–83.
- [25] Frederic, B. and Alain, F., 1999, Electrophoretic Deposition of Silicon Carbide, *Journal of the American Ceramic Society*, 82(8), 2001–2010.
- [26] Dor, S.; Ruhle, S.; Ofir, A.; Adler, M.; Grinis, L. and Zaban, A., 2009, Core/CdS quantum dot/shell mesoporous solar cells with improved stability and efficiency using an amorphous TiO_2 coating, *The Journal of Physical Chemistry*, 113 (9), 3895-3898.
- [27] Lessing, P., Erickson, A., Kunerth D., 2000, Electrophoretic deposition [EPD] applied to reaction joining of silicon carbide and silicon nitride ceramics, *Journal of Materials Science*, 35, 2913–2925.
- [28] Kok-Tee, L., Sorrell, C., 2013, Effect of Charging Agents on Electrophoretic Deposition of Titanium Particles, *Journal of the Australian Ceramic Society*, 49(2), 104 – 112.
- [29] Murgulescu, I. and Radovici, O., 1961, 2nd International Congress on Metallic Corrosion, London, 10-15, April, Butterworths, London, 202-205.